# Design of VIRTUOSE 3D : a new haptic interface for teleoperation and virtual reality

**Florian GOSSELIN** **Alain RIWAN**

Department of Intelligent Systems Technologies – Robotics and Interactive Systems Unit
Commissariat à l'Energie Atomique – Laboratory of Technologies and Systems Integration
BP6 – 92265 Fontenay aux Roses Cedex – France
florian.gosselin@cea.fr alain.riwan@cea.fr

**Abstract**

*Taking advantage of its long experience in the field of nuclear teleoperation, the CEA has recently developed Virtuose 3D, a new input device for teleoperation and virtual reality. This device is a 6DOF input / 3DOF output haptic device. It introduces different mechanical ameliorations over the existing ones and exhibits particularly good performances. This article presents its design and specifications.*

## 1. Introduction

The CEA began to develop mechanical master slave systems for the nuclear industry in the sixties. In the seventies, it introduced the MA23 master and slave servo controlled arms [1]. In the eighties, the master slave coupling scheme evolved from direct to resolved. This evolution allowed to introduce amplification ratios, re-indexing and later more advanced functions like shared control and virtual mechanisms, leading in the nineties to computer assisted teleoperation [2]. It was then possible to think about the development of new master and slave arms as independent systems with different sizes and capacities. The first step was made on the slave side by using either a 7DOF dextrous arm developed at CEA [3] or a conventional Staübli RX90 industrial robot [4] as slave arms. The second step consisted in developing new input devices.

Since the design of the MA23, a very large number of input devices were developed for different applications from heavy teleoperation to delicate telesurgery. Some of the most significant ones are the JPL Model C and Model X which are two of the first universal master arms [5], the Haptic Master developed by Professor Iwata [6] and the BSP developed at AEA [7] which exhibit a parallel structure, the PHANToM first developed at MIT and now sold by Sensable Technologies, Inc. [8] [9] which is particularly well adapted for haptic interaction with virtual environments and finally the Freedom 6S developed by professor Hayward [10] which is particularly sensitive.

In spite of their respective merits, all of these arms exhibit important drawbacks, having either a limited rotational workspace and / or a limited amount of force feedback. This led us to develop a new input device. As it is our field of application, this master arm was designed for nuclear and off-shore teleoperation. Its specifications are given in section 2 and its design is presented in section 3. The results obtained were used to develop Virtuose 3D, a 6DOF input / 3DOF output patent pending master arm described in section 4.

## 2. Specifications of a new master arm for teleoperation

A large consensus exists on the characteristics a 'good' input device must exhibit [8] [11] [12] [13] [14] [15] [16]. Whether considering virtual reality, telesurgery or heavy arms teleoperation, all authors have the same conclusions. A 'good' master arm must satisfy three types of criteria :

- **Performance criteria :** Ideally, a master-slave system must be 'transparent'. The operator must have the feeling that he performs the task directly in the remote environment. He must be free in unencumbered space (which requires a large and singularity free workspace, low inertia and low friction) and must feel crisp contacts against the obstacles encountered by the slave arm (which requires a sufficient force feedback, a high bandwidth and a large stiffness).
- **Integration criteria:** The master arm must be compact enough to be easily integrated in a workstation.
- **Maintainability criteria :** The master arm must be designed as much as possible with off the shelf components in order to minimize cost and simplify maintenance.

All existing input devices were designed using these qualitative criteria. They exhibit, however, very different performances [5] [17] [18] [19] and are therefore more or less adapted to different applications. It is however essential in the design phase of an input device to know if it will fit a particular task efficiently. Precise requirements must thus be associated with each criterion.

These requirements concern the master arm and its control board, which drives data transmission between the operator and the slave arm (these data can eventually be amplified or reduced). The specified level of performance must take advantage of the best operator's and slave arm's capacities within the limits of the desired tasks. This issue requires a correct understanding of these capacities. To obtain the operator's manipulative abilities, we used many sources of information coming either from medical science, ergonomics or robotics. Keeping in mind that the new master arm has to be used for nuclear and off-shore teleoperation, we made the assumption that the operator is seated in a cabin and manipulates the master arm with a joystick handle as a grip. To obtain the requirements on the slave side of the system, we considered, as a reference, an electric slave arm whose specifications correspond roughly to the performances of the Staübli RX90 industrial robot used as a slave arm for nuclear teleoperation in CEA.

Using this information and considering a passive bilateral coupling scheme (both arms are reversible and torque controlled), we obtained the specifications listed in table 1 [20].

| | |
|---|---|
| Workspace | 300mm |
| Position resolution | 60µm |
| Force capacity | 40N |
| Force resolution | 0.4N |
| Apparent mass | 500g |
| Electric stiffness | 5000N/m |
| Bandwidth | 16Hz |

*Table 1 : Specifications of the new input device*

These specifications take two types of limitations into account :

- **Intrinsic limitations due to the operator's capacities :** As it is driven by a human operator, the master arm must be ergonomic and safe. Its workspace and force range are thus directly determined by the capacity of the operator, while its position and force resolution are closely related to them. On the one side, the ability of the master arm to generate movements or forces below the level of detection of an operator is useless but all significant information coming from the slave must be felt by the operator. On the other side, all the operator's voluntary movement or force must be measured but the operator's hand tremor computed on the slave side must be in accordance with the precision needed to perform all desired tasks with the slave arm.
- **Limitations due to the master-slave system's characteristics :** Besides the previous constraints, the master arm must be designed in accordance to the slave arm. Its position resolution must be high enough to restitute all information coming from the slave to the operator. Moreover, its friction (implicitly associated with force resolution), mass and inertia must be low enough for the master slave system to be comfortable on the master side and performant on the slave side. Conversely, its electric stiffness (the gains of its control loops) must be tuned according to the slave's one so that the limits of stability of the slave are always reached before the limits of the master. Finally, its direct force and position bandwidths must be high enough for the system to follow the operator's motor dynamics and to transmit all of his orders to the slave arm and its inverse bandwidths must be higher than the sensitive bandwidth of the operator (considering the limitations introduced by the slave).

# 3. Design of a new master arm for teleoperation

## 3.1. Introduction

Once specified, the new input device must be designed according to these specifications. Although a 6DOF input / 6DOF output master arm is a priori necessary to control a 6DOF slave robot, we first designed a 3DOF input / 3DOF output one. In fact, such a 3DOF structure can be used as the basis of a 6DOF input device, being either serial as the MA23 of parallel as the Haptic Master.

The design of a robot and its optimisation are quite complex problems as results depend on the parameters taken into account. In this article, we will optimise the workspace of the robot, its static force capacity, its apparent stiffness and its apparent mass. The same criteria were used to design the MA23 [21].

As the position and force resolution of the master arm depends directly on the choice of encoders and motors and on the quality of the fabrication that introduces variable clearances and frictions in the structure, they will not be studied here. Moreover, as the bandwidth depends directly on the stiffness and on the mass of the robot, it will neither be optimised.

## 3.2. Modelling tools

The first design driver taken into account is the workspace of the robot. It is defined as the set of configurations (only positions here) the robot can reach. To study this parameter, we will scan the Cartesian space and check which positions the robot can effectively reach using its inverse geometric model that can be written :

$$q=g(X) \tag{1}$$

This model is used to tune the size of the robot until its workspace encompasses the cube of 300mm specified in table 1.

The second design driver we must consider is the force capacity of the robot. It is defined as the minimum amount of force it can apply in any direction. To study this parameter, we will use the notion of force ellipsoid defined as the operational forces produced by 1 N.m motor torques. Calling $J_{mot}$ and $G_{mot}$ the direct and inverse Jacobian matrices from motor to operational space, this ellipsoid can be defined by the following equation :

$$F^T.(J_{mot}.J_{mot}^T).F \leq 1 \tag{2}$$

It allows to compute for each reachable configuration the minimum force the robot can apply in all directions. It is used to tune the reduction ratios until this force is equal to 40N as specified in table 1.

The third design driver taken into account is the master arm's electric stiffness. It is defined as the minimum static gain in any direction deduced in the operational space from the maximum stable static gain of the motor's control loops. To study this parameter, we will use the notion of apparent stiffness ellipsoid defined as the operational forces produced by a 1 meter operational displacement. Calling $K_{mot}$ the motor static gain ( $\tau_{mot}=K_{mot}.dq_{mot}$ ), this ellipsoid can be defined as follows :

$$F^T.(K.K^T)^{-1}.F \leq 1 \tag{3}$$

With the apparent stiffness matrix $K=G_{mot}^T.K_{mot}.G_{mot}$. This ellipsoid allows to compute for each reachable configuration the minimum apparent stiffness in all directions. It is used to tune the reduction ratios until this stiffness is equal to 5000N/m as specified in table 1.

Finally, the fourth design driver taken into account is the apparent mass of the robot. It is defined as the maximum mass experienced in all directions by the operator when moving the end tip of the robot in free space (the motor torques are nullified in this case). To study this parameter, we will use the notion of apparent mass ellipsoid defined as the operational forces produced by a 1 m/s$^2$ operational acceleration. Calling $A_{mot}(q)$ the kinetic energy matrix of the robot, this ellipsoid can be defined by the following equation :

$$F^T.(M.M^T)^{-1}.F \leq 1 \tag{4}$$

With the apparent mass matrix $M=G_{mot}^T.A_{mot}(q).G_{mot}$ that takes inertia of the links of the robot, of its end tips modelled as a punctual masses, of the motors and of the rotors of the motors into account computed under the following simplification assumptions. The centrifugal and Coriolis forces are neglected as the end tip of the robot manipulated by the operator experiences relatively small speeds. The gravity forces are also neglected as the master arm will be statically balanced. The simplified dynamic model of the robot can thus be written $\tau_{operator}=A_{mot}(q).\ddot{q}_{mot}$ in motor space. It can be written $F_{operator}=G_{mot}^T.A_{mot}(q).G_{mot}.\dot{V}$ in operational space if we neglect the terms involving the velocity in the dynamic model derived from the inverse kinematic model.

This ellipsoid allows to compute for each reachable configuration the maximum apparent mass in all directions. It is used to optimise the size of the robot in order to minimise this maximum mass.

## 3.3. Optimisation scheme

The parameters of our optimisation problem are the size of the robot that determines its workspace and the reduction ratios that determines its force capacity and apparent electric stiffness. The optimised criterion is the apparent mass that is the most binding constraint [22]. For each of the competing structures, the following procedure is applied :

1. For different sizes of the robot, its total workspace is computed using its geometric model. If this workspace is smaller than specified, this geometry is excluded. Else the following steps consider each possible position of the useful cubic workspace specified in table 1 in the total workspace computed here.
2. For each position of the useful workspace, the reduction ratios necessary to obtain a sufficient force capacity and a sufficient apparent stiffness are computed. As it is important to obtain warranted performances all over the useful workspace of the robot, the values computed take the worst case in all directions and all over the useful workspace into account.
3. For each position of the useful workspace, the apparent mass of the robot is computed taking the reduction ratios from step 2 into account. Here again, the maximum mass in all directions and all over the useful workspace is taken into account.
4. For each size of the arm, the useful workspace that minimises the maximum apparent mass is retained as the optimum useful workspace. The reduction ratios corresponding to this geometry are directly deduced from step 2.
5. The optimum size of the arm is the size that gives the best compromise between performances (minimum apparent mass) and compactness (small size of the arm).

Once this procedure has been applied to each of the competing structures, it is possible to compare their respective merits. To give sense to this comparison, these structures must be based on the same technological components. In particular, we will assume the use of a Brushless DC motor whose specifications are given in table 2. We will also assume the use of capstan cable reducers as they minimise clearances and friction. Finally, we will suppose that the robots are composed of aluminium bars with linear mass of 150g/m with 40g end tips at each extremity.

| | |
|---|---|
| Rated torque | 0.318 N.m |
| Maximum torque | 0.955 N.m |
| Rotor inertia | 0.0364 kg.cm$^2$ |
| Maximum control gains | 1.75 N.m/rad |
| Mass | 500 g |

*Table 2 : Motor specifications*

## 3.4. Candidate solutions

Most of existing master arms make use of a four bar mechanism serially connected to a rotational axis either as a positioning stage if serial or as a sub-structure if parallel. This simple and efficient solution allows to design 3DOF arms with motors close to the base thus reducing inertia. We will therefore limit our study to this type of structures. Purely serial solutions will be excluded because of the necessary use of carried motors or complex transmissions to actuate the joints remote from the base. The first solution increases the apparent mass while the second one decreases the mechanical stiffness and increases the complexity. Purely parallel solutions will be also excluded because they are relatively complex and encumbering.

Six such 3DOF structures with motors fixed or close to the base will be considered in this article. To further reduce the inertia of the robot, the four bar mechanism will be made of strong cables instead of rigid bars whenever possible (on all structures but the Cartesian actuated one).

- **Decoupled actuation scheme with Fixed Motors (DFM) :** The first solution to obtain such a 3DOF structure is to have all motors fixed on the base. Their movement can be transmitted to the joints of the robot with cables as on the MA23. These cables have to be thiner than the structural cables of the four bar mechanism as they need to be routed along complicated paths that depend on the configuration of the robot (fortunately, the use of a four bar mechanism allows the movement of the third motor to be transmitted with these thin cables only up to the second joint). This solution is illustrated by figure 1.

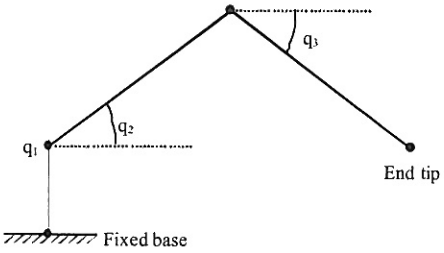


*Figure 1 : DFM 3 DOF structure*

- **Decoupled actuation scheme with Mobile Motors (DMM) :** The previous solution is quite obvious but it introduces long, thin cable paths and thus flexibility and complexity. To avoid this drawback, the second and third motors can be fixed on the first link of the robot as for example on the PHANToM Desktop. Although these motors are no longer fixed on the base, they stay close to it and thus introduce only little inertia. This solution is illustrated by figure 2.

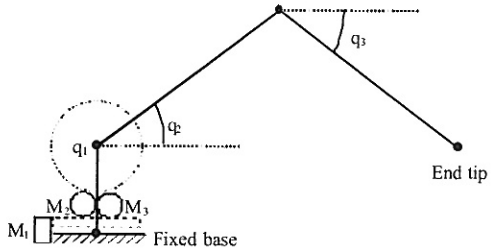


*Figure 2 : DMM 3 DOF structure*

- **Decoupled actuation scheme with Balancing Motors (DBM) :** The previous solutions allow minimization of the moving mass of the structure but are not statically balanced. To avoid this drawback, the second and third motors can be fixed directly on the second and third link of the robot to statically balance the structure. This solution, illustrated by figure 3, is used for example on the PHANToM Premium [8].

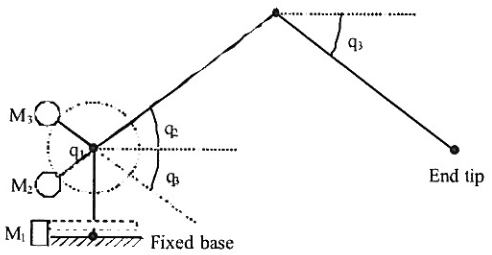


*Figure 3 : DBM 3 DOF structure*

- **Coupled actuation scheme with Fixed Motors (CFM) :** Previous solutions have either complicated cable paths or moving motors. To avoid these problems, the North Western University proposed an original solution illustrated by figure 4 [23]. The three motors are fixed on the base. Their movements are transmitted to the articulations of the robot either with conventional reduction means on axis 1 or with conical reduction means on axes 2 and 3. Couplings are thus introduced between the three axes of the robot. According to the technical solutions used, these couplings can be either identical (ICFM if motors 2 and 3 rotate in the same direction as the first axis of the robot rotates) or opposite (OCFM if they rotate in opposite directions under the same conditions).

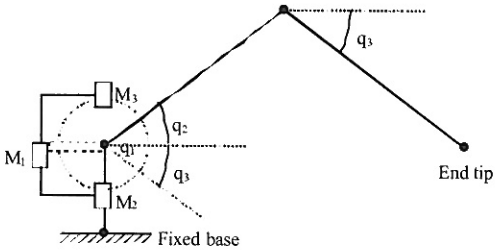


*Figure 4 : CFM 3 DOF structure*

- **CARtesian actuation scheme (CAR) :** The previous structures use the parallelogram as a movement generator. It can also be used as a movement amplifier. This solution, illustrated by figure 5, was used for example on the Toshiba Master Arm [12]. The movements are generated by a 1DOF and a 2DOF Cartesian sub-structures and then amplified by the parallelogram.

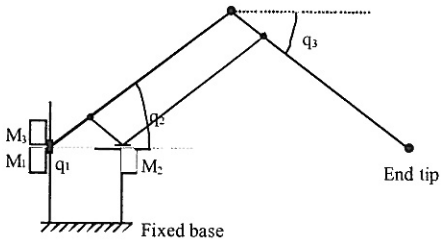


*Figure 5 : CAR 3 DOF structure*

## 3.5. Optimisation results

The previous architectures were optimised according to the optimisation scheme given in section 3.3. The results obtained for the DMM 3DOF structure are given on figure 6. The minimum value (over all possible positions of the useful workspace) of the maximum apparent mass of this robot (over the 30cm cubic useful workspace) is given as a function of its size. The contribution of the structure elements, of the moving motors and of the rotors to this total mass are also given.

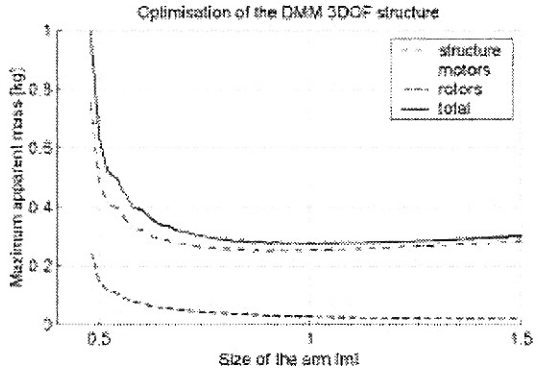


*Figure 6 : Optimisation of the DBM 3 DOF structure*

The minimal mass is obtained when both arm and forearm are 50cm long. However, the decrease is insignificant for lengths above 35cm. This value is thus chosen as the best size considering performances and compactness.

The values obtained for the other structures are given in table 3. The size of the workspace is not given. For each structure, it is more than 300mm×300mm×300mm as specified in table 1. In the same way, the force capacity and the apparent electric stiffness are not given. For each structure, it is more than 40N and 5000N/m in all directions and all over the useful workspace as specified in table 1.

| | Arm size | Reduction ratios | | Max. mass |
|---|---|---|---|---|
| DFM | 35cm | $r_1$ =33.1 | $r_{23}$=24.1 | <319g |
| DMM | 35cm | $r_1$ =33.1 | $r_{23}$=24.1 | <319g |
| DBM | 35cm | $r_1$ =33.1 | $r_{23}$=24.1 | <540g |
| ICFM | 29cm | $r_1$ =50 | $r_{23}$=30 | <634g |
| OCFM | 35cm | $r_1$ =48.6 | $r_{23}$=36 | <393g |
| CAR | 35cm | $r_1$ =$r_2$ =200 | $r_3$ =146.6 | <488g |

*Table 3 : Optimised 3 DOF structures*

According to these results, the best structures are the DFM and DBM. Their maximum apparent mass over a 30cm cubic workspace is less than 320g in all directions. Although the DMM has more mobile parts than the DFM, its maximum apparent mass is the same because its extra mass coming from the mobile motors does not act in the same direction as the mass coming from the elements of structure. Moreover, the DMM structure is mechanically more simple than the DFM as it does not need complicated cable paths. This is the best choice for a new teleoperation master arm.

The other structures exhibit noticeably worst performances. For the DBM and CAR structures, the additional mass comes from extra moving parts, either mobile balancing motors for the DBM or structure elements for the CAR. In fact, the CAR structure requires the use of rigid bars to close the four bar mechanism while the other structure can use a lighter cable connection. Moreover, it requires an additional Cartesian stage that also introduces extra mass. For the ICFM and OCFM, the extra mass comes from kinematic inefficiency. This inefficiency is due to the couplings introduced between the first and second and third axes. These couplings call for larger reduction ratios in order to satisfy the force and stiffness requirements, which in turn lead to a larger apparent mass.

### 3.6. Summary

In this section, we presented six candidate solutions for the development of a new master arm for teleoperation and demonstrated that the most promising competitor is the 3DOF structure with decoupled actuation scheme with mobile motors.

The results obtained exhibit however large reduction ratios, typically more than 20. Such large ratios cannot be easily obtained in a small volume using capstan cable reducers as we wanted to use. To answer this problem, we decided to conduct additional research in two directions. On the one hand, we studied an new patent pending actuation scheme based on highly reversible large reduction ratio reducers that will be presented in a foregoing article. On the other hand, we developed an new input device based on the DMM structure but with smaller reduction ratios to confirm and support its theoretically good performances and to test other mechanical ameliorations.

## 4. Development of a new input device based on DMM structure

The previous results were used to develop a new input device based on a decoupled actuation scheme with mobile motors. This patent pending device, called Virtuose 3D, is illustrated by figure 7. Both arm and forearm are 35 cm long according to the results given in table 3. However, the reduction ratios were decreased to

allow the use of capstan reducers. In fact, the specified amount of force can only be obtained at the center of the useful workspace. Moreover, a passive wrist was added to the 3DOF structure in order to obtain a 6DOF master arm.

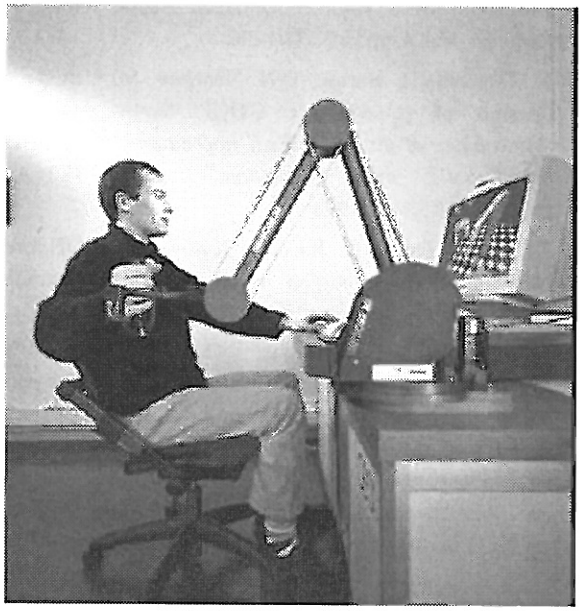

*Figure 7 : Virtuose 3D*

The main features of this 6DOF input / 3DOF output master arm are the following :

- Its structure is decoupled due to the use a centered wrist. This property allows ergonomic one hand operation as no cross-coupling between translations and rotations appears when moving the arm in free or encumbered space.
- The first axis of the wrist is maintained in an horizontal orientation without regard to the configuration of the arm. This property allows a warranty that no singularity will appear anywhere in the translational workspace as long as the grip is rotated less than 90°.
- The arm and forearm are statically perfectly balanced using spiral springs. Virtuose 3D is thus less tiring and intrinsically safe.

Its specifications are summarised in table 4. Although its useful workspace is reduced to the cube specified in table 1, its total workspace is far bigger when considering its more distant points. The force capacity, friction and stiffness are given at the center of the useful workspace (the minimum and maximum values in the reference Cartesian directions are given).

| | |
|---|---|
| Total workspace | 420x490x920 mm |
| Useful workspace | 300x300x300 mm |
| Rated force capacity | 11 to 18 N |
| Maximum force capacity | 34 to 55 N |
| Friction | 0.3 to 0.6 N |
| Electric stiffness | 2350 to 6000 N/m |
| Mechanical stiffness | 3650 to 7500 N/m |

*Table 4 :Specifications of Virtuose 3D*

To date, this arm has not been coupled to a real slave arm. However, the modifications introduced over the theoretical results obtained for teleoperation and given in table 3 make it particularly suitable for haptic interaction with virtual environments. This type of application was therefore favoured and this arm was used to control virtual robots.

To the operator, it appears highly transparent. Friction and inertia are small enough to feel unencumbered space as free. Stiffness and force capacity are high enough to feel crisp contacts with the environment. These properties confirm the theoretical results given in table 3.

## 5. Conclusions

In this article, we presented the activities conducted at CEA toward the development of new input devices for teleoperation and virtual reality. We first presented the specifications of new master arms for teleoperation. Then we presented a comparison of candidate mechanical architectures chosen to answer these specifications. Finally, we presented Virtuose 3D, a patent pending new input device developed according to these results which exhibits particularly good performances. Future work concerns patent pending new actuation schemes and new 6DOF input / 6DOF output structures.

## References

[1] J. Vertut, P. Coiffet, 'Les robots - Tome 3a : téléopération, évolution des technologies', Hermès Publishing, Paris, 1984

[2] L.D. Joly, 'Commande Hybride Position / Force pour la Téléopération : une approche basée sur des Analogies Mécaniques', Ph.D. diss. (in French), University of Paris 6, 1997

[3] P. Desbats, R. Cammoun, F. Littmann, T. Jouan de Kervanoel, J.M. Idasiak, C. Andriot, 'Development of a new dextrous arm for telerobotic maintenance of nuclear facilities', *Proceedings of the ANS 8th Topical Meeting on Robotics and Remote Systems*, Pittsburgh, USA, April 1999

[4] P. Desbats, C. Andriot, P. Gicquel, Y. Soulabaille, C. Souche, 'Force-feedback teleoperation of industrial robots for telerobotic maintenance of nuclear plants', *Proceedings of the 27th International Symposium on Robotics*, Birmingham, UK, April 1998

[5] D.A. McAffee et P. Fiorini, 'Hand Controller Design Requirements and Performance Issues inTelerobotics', *ICAR 91, Robots in Unstructured Environments*, Pisa, Italy, pp186-192 ,June 1991

[6] H. Iwata, 'Pen-based Haptic Virtual Environment', *Proceedings if the 1993 IEEE Virtual Reality Annual International Symposium, VRAIS'93*, Seattle, pp287-292, 1993

[7] M.H. Brown et J.D. Asquith, 'A Man-Machine Interface With Feeling', *Service Robot*, Vol. 2, 1996

[8] T.H. Massie, J.K. Salisbury, 'The PHANToM haptic interface : a device for probing virtual objects', *Proceedings of the ASME Winter Annual Meeting, Symposium on Haptic Interfaces for Virtual Environment and Teleoperator Systems*, Chicago, November 1994

[9] E. Chen, 'Six Degree-of-Freedom Haptic System For Desktop Virtual Prototyping Applications', *Premières Rencontres Internationales de la Réalité Virtuelle de Laval, Actes du colloque scientifique international : Réalité Virtuelle et prototypage*, Laval, France, pp97-106, June 1999

[10] V. Hayward, P. Gregorio, O. Astley, S. Greenish, M. Doyon, L. Lessard, J. Mac Dougall, I. Sinclair, S. Boelen, X. Chen, J.-P. Demers, J. Poulin, I. Benguigui, N. Almey, B. Makuc, X. Zhang, 'Freedom 7 : A High Fidelity Seven Axis Haptic Device with Application to Surgical Training', *Experimental Robotics 5, The Fifth International Symposium*, Barcelona, Catalonia, pp,445-456 June 1997

[11] P.A. Millman, J.E. Colgate, 'Design of a Four Degree-of-Freedom Force-Reflecting Manipulandum with a Specified Force/Torque Workspace', *Proceedings of the 1991 IEEE International Conference on Robotics and Automation*, Sacramento, California, pp1488-1493, April 1991

[12] N. Matsuhira, H. Bamba, M. Asakura, 'The development of a general master arm for teleoperation considering its role as a man-machine interface', *Advanced Robotics*, Vol. 8, no 4, pp443-457, 1994

[13] R.E. Ellis, O.M. Ismaeil, M.G. Lipsett, 'Design and Evaluation of a High-Performance Haptic Interface', *Robotica*, Vol. 4, pp321-327 1996

[14] Y. Tsumaki, H. Naruse, D.N. Nenchev, M. Uchiyama, 'Design of a compact 6-DOF haptic interface', *Proceedings of the 1998 IEEE International Conference on Robotics and Automation*, Louvain, Belgium, pp2580-2585,May 1998

[15] K. Young Woo, B.D. Jin, D.S. Kwon, 'A 6-DOF force reflecting hand controller using the fivebar parallel mechanism', *Proceedings of the 1998 IEEE International Conference on Robotics and Automation*, Louvain, Belgium, pp1597-1602, May 1998

[16] R. Baumann, R. Clavel, 'Haptic interface for virtual reality based minimally invasive surgery simulation', *Proceedings of the 1998 IEEE International Conference on Robotics and Automation*, Louvain, Belgium, pp381-386, May 1998

[17] G.W. Köhler, 'Typenbuch der Manipulatoren - Manipulator Type Book', Thiemig Taschenbücher, Verlag Karl Thiemig, München, 1981

[18] G. Burdea, P. Coiffet, 'La réalité virtuelle', Hermès Publishing, Paris, 1993

[19] L. Stocco et S. E. Salcudean, 'A Coarse-Fine Approach to Force-Reflecting Hand Controller Design', *Proceedings of the 1996 IEEE International Conference on Robotics and Automation, Minneapolis*, Minnesota, April 1996

[20] F. Gosselin, 'Développement d'outils d'aide à la conception d'organes de commande pour la téléopération à retour d'effort', Ph.D. diss. (in French), University of Poitiers, June 2000

[21] J. Vertut, A. Liégeois, 'General Design Criteria for Manipulators', *Mechanism and Machine Theory*, Vol. 16, pp65-70, 1981

[22] V. Hayward, J. Choski, G. Lanvin, C. Ramstein, 'Design and Multi-Objective Optimization of a Linkage for a Haptic Interface', *Advances in Robot Kinematics and Computationed Geometry*, pp359-368, 1994

[23] D.T. Burns, 'Design of a six degree of freedom haptic interface', Master of Science in Mechanical Engineering, Northwestern University, Department of Mechanical Engineering, August 1996